14B.6

EVALUATION OF OPERATIONAL WEATHER RADAR RAIN ESTIMATES IN FLOOD-PRONE AREAS OF CALIFORNIA

Sergey Y. Matrosov[1], F. Martin Ralph[2], Paul J. Neiman[2], and Allen B. White[3]

[1]Cooperative Institute for Research in Environmental Sciences,
University of Colorado and NOAA ESRL, Boulder, Colorado
[2] Scripps Institution of Oceanography, LA Jolla, CA
[3]NOAA Earth System Research Laboratory, Boulder, Colorado

1. INTRODUCTION

It has been recognized that coverage of the operational S-band (wavelength λ~10 – 11 cm) Weather Surveillance Radar-1988 Doppler (WSR-88D) network for quantitative precipitation estimation (QPE) over the coastal western United States has significant limitations and "gaps" (e.g., Westrick et al. 1999). In addition to the large distances between WSR-88D sites in many important coastal areas, gaps in operational radar coverage are also often caused by the blockage of radar beams by mountainous terrain at lower radar tilt (elevation) angles (e.g., Miller et al. 2010). This necessitates the use of higher tilts, which often causes overshooting of shallow rainfall or sampling higher regions of precipitating clouds resulting in biased rain accumulation estimates from operational radar data.

While it is generally believed that the northern Sonoma County, which is in the flood-prone area, lacks adequate WSR-88D coverage, the extent to which operational radar data can be used in this area is not exactly known. The main objective of this study was to quantify the performance of operational radar-based QPE for different rainfall types using available long-term gauge measurements supported by collocated and simultaneous observations of precipitation regimes. Such measurements are available from a site located near Cazadero (CZD) (38.6107°N, 123.2153°W, 478 m MSL) where NOAA's Hydrometeorology Testbed has operated an S-band vertical profiling radar (S-PROF; White et al. 2000) and a collocated precipitation gauge (0.01-inch resolution) for several years. The S-PROF provides high resolution measurements of vertical profiles of equivalent radar reflectivity, Z_e, and vertical Doppler velocity, W. These profiles allow detailed classification of precipitation types and their vertical structure using the approaches described by White et al. (2003). This site is near the Russian River basin in a "gap" area, where WSR-88D coverage is often not available at altitudes less than about 3 km MSL.

This study takes advantage of the analysis by Ralph et al. (2013) of precipitation events observed during landfalling atmospheric rivers (ARs), which are relatively narrow bands of enhanced water-vapor transport associated with extratropical cyclones. AR events observed during only about 1500 hours are responsible for more than half of the total CZD six-year (fall 2004 - summer 2010) precipitation.

Corresponding author address: Sergey Matrosov, R/PSD2, 325 Broadway, Boulder, CO 80305, email: sergey.matrosov@noaa.gov

2. OBSERVATIONAL DATA SETS

The 1500 hours of precipitation observed during AR events were chosen for the analysis. The WSR-88D data used were those from the KMUX radar located at about 199 km to the south-east of CZD. This radar provides unobstructed view of the area of interest using the lowest beam tilt of 0.5°. In addition to the KMUX data, QPE retrievals from the closest WSR-88D KDAX radar were also analyzed. While this radar is the closest to the area of interest (~134 km), its view at the lowest tilt is blocked by the coastal mountains. As shown in Fig.1 the 1.5° tilt is not generally blocked, so this tilt KDAX data were used in this study.

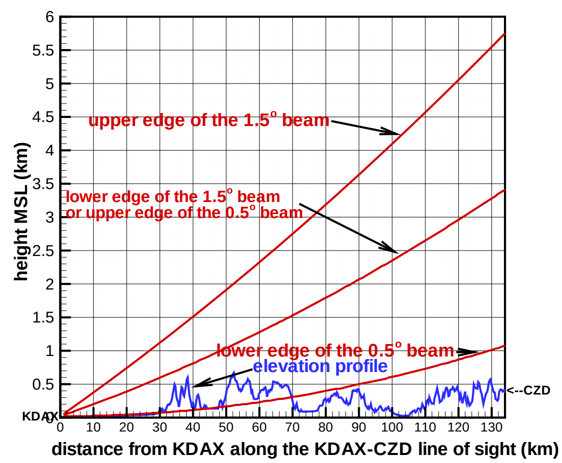

FIG.1. *Terrain elevation profile (blue) and 0.5° and 1.5° beams in the direction from KDAX to CZD.*

S-PROF measurements at CZD were used to classify rain types during the WSR-88D observations. The classification included 7 precipitation types: (1) bright-band (BB) rain; (2) non-bright-band (NBB) shallow rain observed at the ground but not "seen" by the WSR-88D radars; (3) NBB high rain, which was detected by the scanning radars; (4) NBB convective rain; (5) virga detected as rain by operational radars but not providing rain at the ground; and (6) erroneous rain when operational radars detected virga or high clouds but accumulation at the ground resulted from shallow rain. Unlike NBB rain, the BB rain type was almost always detected by the operational weather radars.

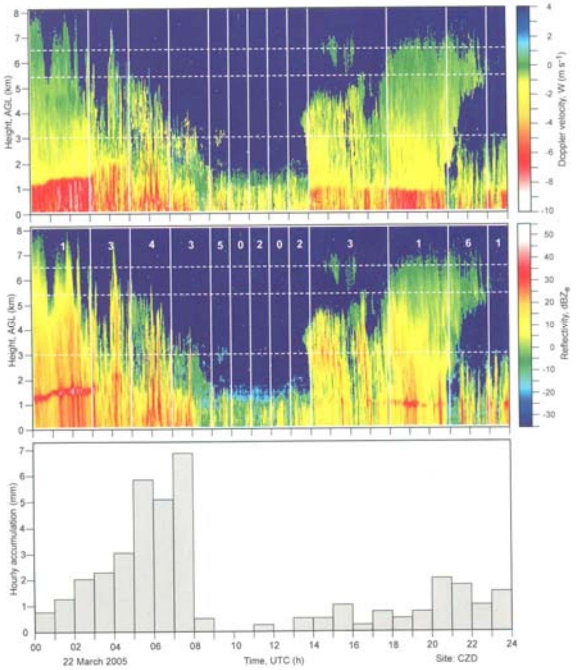

FIG.2. *An example of rain type hourly classification (white numbers with 0 corresponding to no detected rain by both gauge and radar) for an event of 22-MAR-05 based on S-PROF Doppler (upper panel) and reflectivity (middle panel) measurements. Lower panel shows corresponding hourly rain accumulations at the ground.*

The WSR-88D radar resolution volumes in the area of interest are generally higher than the environmental freezing level. The expected lower edges of the 0.5^o KMUX and 1.5^o KDAX beams are at about 3 km AGL height as shown by the lower dashed line in Fig. 2. The middle and upper dashed white lines show the upper edges of those beams for KDAX and KMUX, respectively. The mean vertical profile of reflectivity (VPR) correction found from previous studies was applied to the WSR-88D radar data (Matrosov et al. 2007).

The total accumulation at the CZD ground validation site during ~1500 hours of observations was 4383 mm. While BB rain was observed for about 30 % of all rainy hours, it provided over half (~52%) of all accumulation. The NBB shallow rain was observed at the ground as often as BB rain but it produced less accumulation by a factor of about 4. The convective rain was most intense but it was observed only during approximately 4% of rainy periods. Radar estimates during rain type 5 and 6 resulted in about 5% (each) of the total accumulation.

The performance of different reflectivity – rain rate (i.e., Z - R) relations, including those, which are typically used with WSR-88D measurements, was tested with WSR-88D QPE. On average, the Hydrometeorology TestBed relation $Z = 100\ R^{1.76}$ (Matrosov et al. 2007) provided the best agreement with gauge data at the validation site, so the further illustration of QPE results are given for this relation.

3. EVALUATION OF HOURLY ACCUMULATIONS

Scatter plots of WSR-88D derived hourly QPE estimates for all hourly intervals vs CZD gauge accumulations are shown in Fig.3. The incremental character of gauge data is manifested by the alignment of accumulations along the vertical lines spaced 0.254 mm (0.01”) apart. A group of horizontal points that is aligned horizontally near the X-axis represents the NBB shallow rain, which is not captured in radar observations.

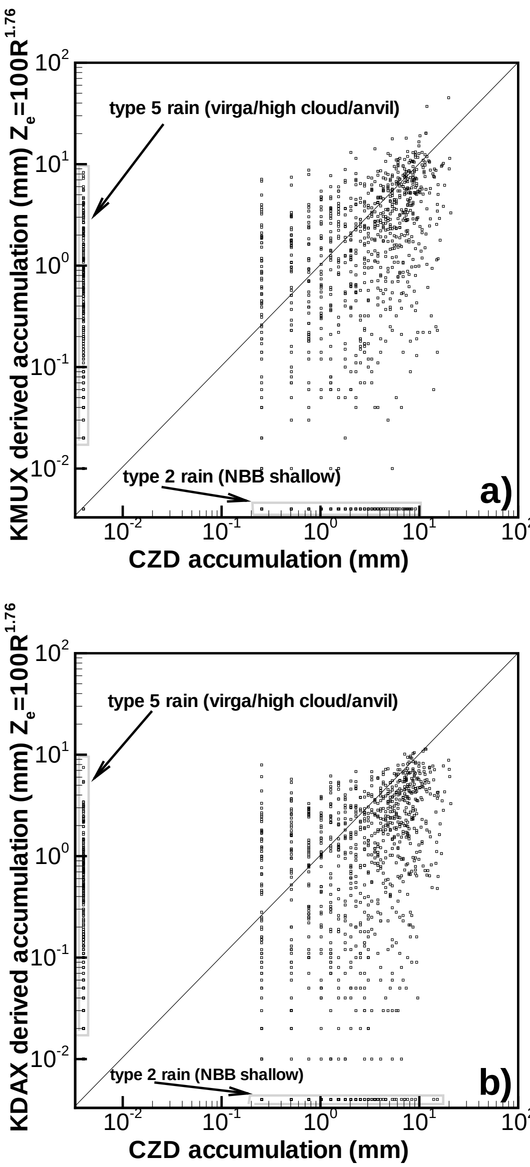

FIG.3. *Scatter plots of all hourly accumulations derived from the CZD gauge and the KMUX (a) and KDAX (b)*

The relative mean biases (RMBs) for KMUX and KDAX QPE estimates are -31% and -51%, respectively. The normalized absolute error (NAE) for both radars is approximately 74% if the climatological mean value of the freezing level (FL) height is utilized in the VPR correction. The use of actual FL heights inferred from simultaneous S-PROF observations improves RMB and NAE values by a few percentage points.

While significant scatter is present when WSR-88D QPE hourly results are compared to gauges for all rain types, a subset of comparisons for BB rain exhibits much better agreement. Figure 4 shows such comparisons.

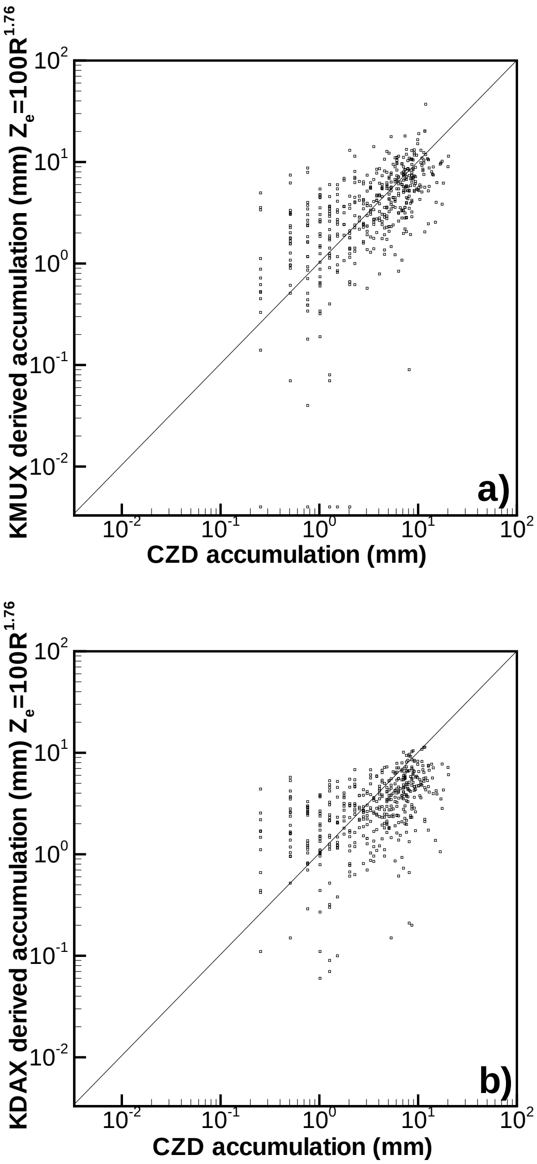

FIG.4. *Scatter plots of all hourly accumulations during BB rain derived from the CZD gauge and the KMUX (a) and KDAX (b)*

The WSR-88D absolute RMB values for BB rain only are generally less than 30% and corresponding NAE values are on the order of 50%. The better agreement (compared to all rainy 1-h intervals) is due, in part, to higher mean echo tops (~7.2 km MSL) compared to the general category of NBB rain (~3.6 km MSL), which results in less severe partial beam filling issues. Another factor for a better agreement is that the standard VPR correction is better suited for stratiform type rains that usually exhibit BB features.

4. EVALUATION OF EVENT TOTALS

In addition to evaluating WSR-88D hourly accumulations, the AR event totals were also analyzed. Overall 58 landfalling AR events were simultaneously observed by WSR-88D radars and the S-PROF. The results of comparisons are shown in Fig. 5.

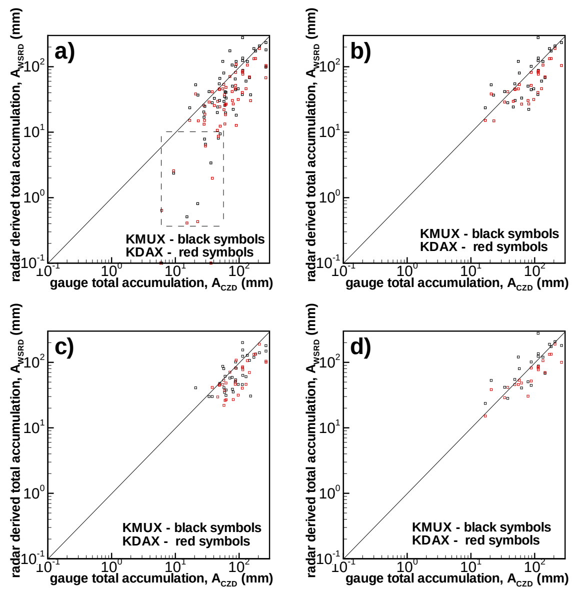

FIG.5. *Scatter plots of event-total radar derived rain accumulations versus gauge data for all 58 AR events (a), for events when BB rain fraction was greater than 33% (b), for events when radar data QPE was greater than 30 mm (c), and for events with mean cloud top heights greater than 5.2 km MSL (d).*

It can be seen from Fig. 5a that for several events (shown inside the dashed line rectangle) WSR-88D severely underestimated total accumulation. These events, however, were not significant (in a relative sense). For those events when WSR-88D total results exceeded 30 mm (Fig. 5c) the agreement with gauge data was relatively good. Almost equally good was the agreement between gauge and radar data for the subset of the events with high fraction of BB rain (Fig.5b) and for the subset of the events with high mean echo tops (Fig.5d) as detected by the S-PROF. The NAE values for these subsets in Figs. 5b-d were around 30-40%.

Better agreement between radar and gauge QPE for event totals (as compared to the hourly accumulations) can be explained, in part, by partial error cancelation incurred during shallow warm rain and virga periods observed during the same event. Note that the S-PROF information is essential for identifying events in subsets shown in Figs. 5b,d. This information is not needed for selecting the event subset in Fig. 5c.

5. KMUX vs KDAX QPE

It can be seen from Figs. 4 and 5 that KDAX derived accumulations are on average smaller than those from KMUX. Figure 6, where accumulations from these two radars are compared, illustrates this fact. The mean bias of KDAX QPE data relative to KMUX is about -25 %. Correlation between KMUX and KDAX results, however, is very high with the correlation coefficient being approximately 0.95 for event totals and 0.8 for hourly accumulations. One plausible explanation of the KDAX-KMUX bias is differences in calibration and unaccounted losses along the propagation paths.

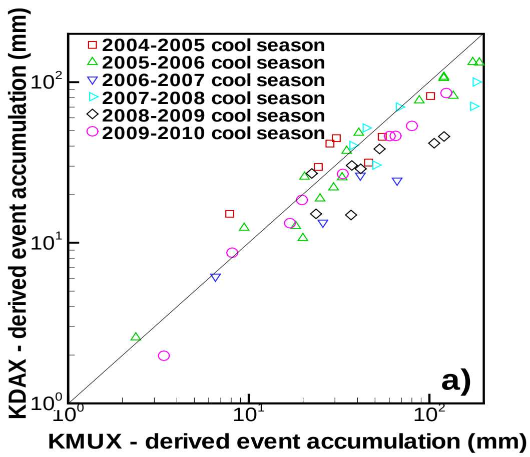

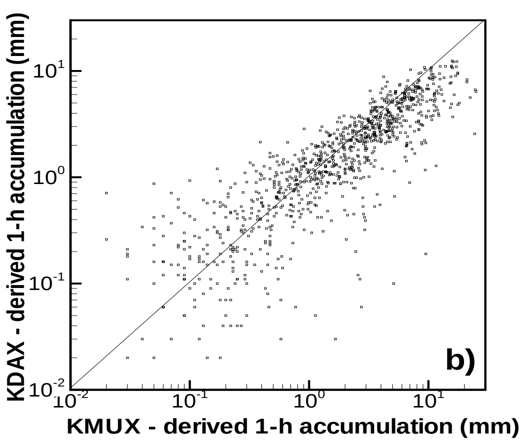

FIG.6. *Comparisons of KMUX and KDAX derived event total (a) and hourly (b) accumulations.*

6. CONCLUSIONS

Analysis of WSR-88D-based QPE results in in a relative coverage “gap” in the flood-prone coastal areas of California’s northern Sonoma county indicated that QPE uncertainties strongly depend on rain type. Results for BB-type rains, which account for more than half of total accumulation, have relatively small mean biases and typical uncertainties of about 50% for 1-hour accumulations and about 35% for event totals. This type rains usually have high echo tops, so partial beam filling issues are relatively small compared to other rain types

Radar QPE biases for NBB rain are significant (~-70- -80%). About 20 % of total rainfall is completely missed by WSR-88D radars(e.g., shallow warm NBB rain) due to overshooting. False WSR-88-based rain (i.e., due detection of virga, anvils or high clouds which are detached from precipitation near the ground) amounts to about 10% of the total ground accumulation.

On average, the WSR-88D results for event totals agree with gauge data better compared to hourly accumulations. Better agreement is present for heavier rainfall events. Partial cancelation of errors is one factor contributing to this better agreement. Complementary information from profilers in the area of interest (e.g., data on FL and echo top heights and VPR shapes) helps to improve WSR-88D QPE.

The lessons learned from the unique data and analysis in the vicinity of the Russian River basin presented here are relevant to many basins along the U.S. West Coast from southern California to Washington State, e.g., the Eel River in California, Nehalem and Smith Rivers of Oregon and the Chehalis River of Washington. Precipitation in these other basins are also dominated by rainfall and their extreme events are associated with atmospheric river conditions (Neiman et al. 2011). They also are affected by the relatively poor coverage from scanning weather radars that is characteristic of the mountainous western US.

REFERENCES

Matrosov, S.Y., K.A.Clark, and D.E. Kingsmill, 2007: A polarimetric radar approach to identify rain,melting-layer and snow regions for applying corrections to vertical profiles of reflectivity. *J. Appl.Meteor.and Climatology*, **46**, 154-166.

Miller, D.A., D. Kitzmiller, S. Wu, and R. Setzenfand, 2010: Radar precipitation in mountainous regions: Corrections for partial beam blockage and general coverage limitations. *24th* 548 *Conf. On Hydrology*, St. Louis, MO, Amer. Meteor. Soc., paper 163622.

Neiman, P.L., G.A. Wick, F.M. Ralph, B.E. Martner, A.B. White, and D.E. Kingsmill, 2005: L. J. Schick, F. M. Ralph, M. Hughes, G. A. Wick, 2011: Flooding in Western Washington: The Connection to Atmospheric Rivers. *J. Hydrometeor.*, **12**, 1337-1358.

Ralph, F.M., T. Coleman, P. Neiman, R. Zamora, and M. Dettinger, 2013: Observed impacts of duration and seasonality of atmospheric-river landfalls on soil moisture and runoff in coastal northern California. *J. Hydrometeor*., in press.

Westrick, K.J., C.F. Mass, and B.A. Colle, 1999: The limitations of the WSR-88D radar network for precipitation measurement over the coastal western United States. *Bull. Amer. Meteor. Soc*., **80**, 2289-2298.

White, A. B., J. R. Jordan, B. E. Martner, F. M. Ralph, and B. W. Bartram, 2000: Extending the dynamic range of an S-band radar for cloud and precipitation studies. *J. Atmos. Oceanic Technol.*, **17**, 1226-1234.

White, A. B., P. J. Neiman, F. M. Ralph, D.E. Kingsmill, and P.O.G. Persson, 2003: Coastal orographic rainfall processes observed by radar during the California land-falling jets experiment. *J. Hydrometeor*. , **4**, 264-282.